Flame flashback critical Damköhler number for CO2 diluted CH4 and C3H8 mixtures with air

Maria Clara de Jesus Vieira, Luis Fernando Figueira da Silva

Flame flashback critical Damköhler number for CO_2 diluted CH_4 and C_3H_8 mixtures with air

Maria Clara de Jesus Vieira[1,2] and Luís Fernando Figueira da Silva[1,2*†]

[1*]Department of Mechanical Engineering, Pontifícia Universidade Católica do Rio de Janeiro, Rua Marquês de São Vicente, 225, Rio de Janeiro, 22.451-900, RJ, Brazil.
[2]Institut Pprime UPR 3346, Centre National de la Recherche Scientifique, 1 Avenue Clément Ader, Futuroscope Chasseneuil, 86961, France.

*Corresponding author(s). E-mail(s): luis-fernando.figueira-da-silva@ensma.fr;
Contributing authors: maria-clara.de-jesus-vieira@ensma.fr;
†These authors contributed equally to this work.

Abstract

The premixed laminar flame flashback phenomenon in tubes has been known and studied for several decades. However, the effect of the CO_2 dilution has not been addressed, which is relevant for assessing the safety of oil-producing facilities. Furthermore, even if numerical studies have underscored the important role played by the mixture Lewis number ($\boldsymbol{Le}$), these lack an experimental validation. For this reason, specific studies of premixed flame flashback in laminar flows have been undertaken. The objective is to assess the flame flashback critical conditions in mixtures of hydrocarbons – methane or propane diluted by various amounts of CO_2 – with air. This is effected by determining the critical Damköhler number, which is computed using both experimental and numerical data. The former leads to the flashback critical velocity gradient, whereas the latter to a characteristic chemical time scale. The effect of different flame thickness definitions on the Damköhler

number ($\boldsymbol{Da}$) is examined, evidencing than an order of magnitude discrepancy may arise depending on the definition choice. For methane/air mixtures the critical $\boldsymbol{Da}$ increases with the equivalence ratio, whereas a decrease of nearly two orders of magnitude has been obtained for propane/air mixtures. The original results show that $\boldsymbol{CO_2}$ dilution increases $\boldsymbol{Da}$ only when the fuel dilution percentage is larger than 25% and 50%, for methane and propane, respectively, situations which correspond to flame extinction after flashback. The propane/air/$\boldsymbol{CO_2}$ mixture results exhibit a $\boldsymbol{Da \propto Le^{5.06}}$ dependency which closely follows the trend computed previously, whereas the methane/air/$\boldsymbol{CO_2}$ results evidence the thermal boundary condition at the tube wall influence.

Keywords: Boundary layer flashback, Flashback propensity, Laminar, Premixed flames

1 Introduction

The flame flashback phenomenon in laminar flows has been known and studied for several decades [1]. A significant amount of results is available, which demonstrate the influences exerted by fuel, dilution and tube diameter choices [2], for instance. However, a recent review of the state of the art [2] indicates that significant knowledge gaps remain, in particular with regard to the combustible mixture Lewis number influence, and the effect of fuel dilution by CO_2. Indeed, concerning the latter, CO_2 is used to displace oil in mature reservoirs, and is naturally found in some geological formations, which leads to fuel gas produced with dilutions that may reach 75 %. Therefore, these knowledge gaps prevent the use of existing results for the prediction of flame flashback, in particular under the CO_2-abundant gas production conditions of the Brazilian pre-salt offshore platforms. For this reason, specific experimental studies of CO_2-diluted hydrocarbon/air premixed flames flashback in laminar flows are undertaken here.

Classically [1], the flame flashback through the boundary layer is assumed to occur when the velocity of flow, $u(y)$, is smaller than the local burning velocity, S_L^0, at some point near the wall, as seen in Fig. 1. The position at which the burning velocity is equal to the flow velocity is defined as the flame penetration distance, δ_p. The flame is supposed to be extinguished at a certain distance from the wall, called the quenching distance (δ_q). When the flow velocity at $y = \delta_p$ is equal to the local burning velocity the critical condition for flame flashback arises. This model further assumes that no flame/fluid interaction occurs and, therefore, that there are no disturbances in the laminar flow velocity upstream to the flame. More recent works determined that flow reversal may occur downstream the flames at the wall vicinity [3, 4].

During the past decades, the critical conditions leading to laminar boundary layer flashback in tubes have been subject of experimental and numerical studies. Pioneering experimental studies [5] have identified the role of the flow

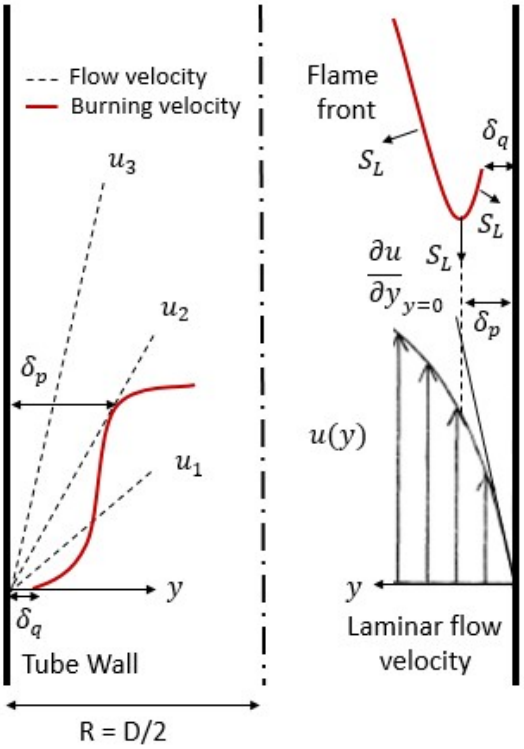

Fig. 1: Schematic model of the interaction between flame and boundary layer that leads to the concept of the critical velocity gradient. Velocity profiles of the laminar flow and flame front under the flashback condition.

velocity gradient at the wall on the flashback onset. The critical value of this gradient has been measured, for instance, as a function of the fuel type, mixture equivalence ratio and oxygen content, and summaries of these results are available [1, 2]. In particular, a decrease in oxygen dilution by nitrogen has been shown to significant increase the flame flashback propensity. Numerical studies of this phenomenon have extended the critical velocity gradient concept by means either of a Damköhler or a Karlovitz number [6–9]. The computed critical Damköhler number has been shown to be an increasing function of the Lewis number, and to decrease when the tube wall boundary condition changes from isothermal to adiabatic. To the best of our knowledge, a systematic experimental investigation of the Lewis number influence on the flashback propensity has not been performed, however. More recently, flame stretch effects were accounted for and shown to decrease the critical bulk velocity for flashback to occur for near-stoichiometry H_2-air flames [10]. However, the stretch influence on flashback was found to be less pronounced

for methane/air flames. Newly proposed Karlovitz number correlations incorporate the stretch effect on a premixed flame to predict the boundary layer flashback of turbulent swirling flames [11, 12].

In order to further define the laminar boundary layer flashback controlling parameters, Fig. 1 shows a schematic model of this process, where a stabilised flame front can be seen inside a tube near the wall. On the right side of this figure, the velocity of the flow, $u(y)$, is represented by a parabolic profile. On the left side of Fig. 1, which considers the stabilised flame front immediately upstream the edge of the tube, represents the three conditions conditions for flame/flow interaction. The horizontal axis, y, represents the distance from the tube wall, and the dashed lines 1, 2 and 3 symbolise different flow velocities. The solid curve represents the velocity of the laminar flame front near the wall. Note that, in this model, the laminar flame front velocity is zero within the quenching region, i.e., $0 < y < \delta_q$. When the flow velocity is greater than the local burning velocity througout the flame front, the flame leaves the tube and stabilises on the outside, a situation which is represented by line 3. Line 2 indicates the critical condition for observing flame flashback, when the flow velocity is equal to the burning velocity at the flame penetration distance, $y = \delta_p$. If the flow velocity is reduced (line 1), the flame propagates into the tube. Given this picture, the velocity gradient used to characterise the flashback in the critical situation may then be defined as

$$g_c = \left(\frac{du}{dy}\right)_{y=\delta_p} = \frac{S_L^0}{\delta_p}. \tag{1}$$

In the classic premixed flame flashback model [1, 2], the local burning velocity at this critical condition is equal to that of a freely propagating one dimensional laminar premixed flame, and the flame penetration distance within the boundary layer, δ_p, that controls the flashback phenomenon, is considered proportional to the laminar flame thickness, i.e., $\delta_p = K\delta_L$, where K is assumed to be constant. This model further supposes that a developed laminar flow exists within the tube, which enables the critical condition for flashback to occur through the boundary layer to be expressed by equating the flow's and the modelled expressions of the critical velocity gradient, i.e., $g_c = (du/dy)_{y=\delta_p} = 8\bar{U}/D = S_L^0/(K\delta_L)$, where D is the tube diameter and $\bar{U}$ is the bulk flow velocity, both which stem from measurements here.

One should note that K may be interpreted as a Damköhler number [6, 7]. The critical Damköhler number for flashback to occur may then written as

$$Da = \frac{S_L^0}{g_c\delta_L} = \frac{DS_L^0}{8\bar{U}\delta_L}. \tag{2}$$

An extra usual assumption concerns the definition of the laminar flame thickness, which is taken to be proportional to the mixture thermal diffusion

coefficient, $\delta_L = \alpha/S_L$, thus leading to:

$$Da = \frac{(S_L^0)^2}{g_c \alpha} = \frac{D(S_L^0)^2}{8\bar{U}\alpha}. \tag{3}$$

However, such a flame thickness definition is known to under-predict the computed thermal thickness of premixed flames [13]. Equations (2) and (3) suggest that, if the Damköhler number critical value is constant, the flashback propensity in terms of the critical velocity gradient should be reduced when S_L^0 decreases, which is the case for hydrocarbon-air CO_2 diluted mixtures of interest to the present work. Note also that, under the assumptions leading to Eq. (3), the critical bulk velocity for flame flashback would be directly proportional to the tube diameter and the squared flame speed, i.e., $\bar{U} \propto D(S_L^0)^2$. As a consequence, the assumption of a constant Damköhler number could lead to an improper safety assessment, in terms of this velocity, if the actual Da value is larger than the presumed constant one.

The goal of this work is thus to determine the influence of the mixture composition and fuel dilution by CO_2 on the flame flashback limit, which is represented by a Damköhler number. This is effected by combining original experimental data of the critical flashback conditions with detailed chemical kinetics computational results to determine the flame speed and thickness. More specifically, the question of whether Da may be assumed to be constant is addressed, as is the influence of the mixture effective Lewis number. The extent to which different flame thickness definitions may change the critical Damköhler number values is examined also.

This paper is organised as follows: the experimental and computational methodologies used to determine the Damköhler and effective Lewis numbers for CO_2-diluted methane and propane mixures with air are first presented. Then is assessed the influence on the Damköhler number of the flame thickness definition, of the mixture equivalence ratio and fuel CO_2 dilution, and of the effective Lewis number. Finally, the main conclusions of this work are presented.

2 Methodology

In this section are presented the experimental and computational methodologies adopted to characterise the flame flashback.

2.1 Experimental methodology

To study the boundary layer flashback phenomenon in laminar flows an experimental bench was set up, which is schematically shown in Fig. 2. Its dimensions were chosen based on data found in the literature [2], which indicated that determining the flashback limits throughout the flammability range of methane and propane mixtures with air should require tubes with different diameters

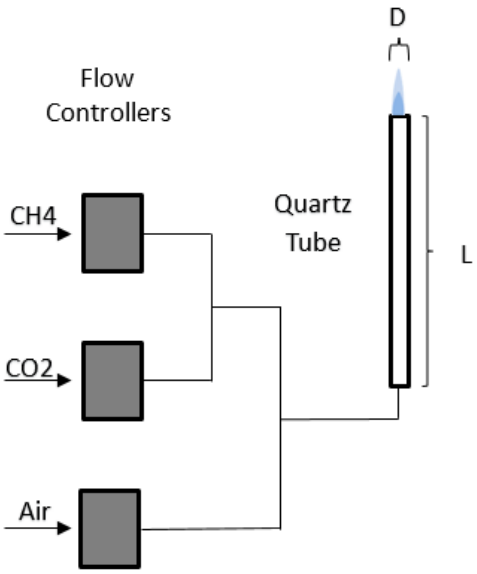

Fig. 2: Experimental apparatus scheme, showing the fuel (CH_4 or propane), air, and CO_2 mass flow controllers, mixing tubes, vertical quartz tube, and flame position prior to flashback.

and a wide range of flow meters. Accordingly, this bench consists of interchangeable $D = 17$, 6, 5, and 4 mm inner diameter quartz tubes, which are vertically mounted, the larger diameters being used to determine the flashback around stoichiometry, and the smaller for either fuel lean or fuel rich mixtures. These tube diameters are known with a 0.6 % accuracy. Note that for tubes with diameters smaller than 2 mm, extinction, instead of flashback, is expected to occur for undiluted mixtures [1]. The tubes have a length L of 1 m, that ensures a fully developed laminar flow for all the Reynolds numbers considered, i.e., $L/D > 0.05\,\mathrm{Re}$. The maximum Reynolds number for all mixtures, flow rates and tube diameters considered is 1,250. This value correspond to an undiluted propane/air mixture, with equivalence ratio of $\phi = 1.25$, flowing through the 17 mm diameter tube.

As shown in Fig. 2, Alicat Scientific flow controllers are used to measure the reactants flow rates prior to mixing. These MC-series controllers, with ranges of 0.5, 5, 50 and 500 SCCM, 5 and 20 SLPM, have a standard accuracy calibration of ± 0.6 % of reading or ± 0.1 % of full scale, whichever is greater. Throughout the experiments performed these flow controllers were used in different gas lines, so as to cover fuel/air mixtures from the lean to the rich flammability limit, and CO_2 dilution in the fuel stream up to 75 %. Mixing is effected in a 6 mm outer diameter tube which

length is at least twice that required for obtaining a fully developed flow. The fuels studied here were methane and propane, which constituents are $C_3H_8/CH(CH_3)_2(C_2H_5)/C_2H_6/1\text{-}C_4H_8/C_3H_6$, and molar basis composition is (89.1, 4.16, 3.12, 2.94, 0.68) %.

Each experiment begins with the flame stabilised at the quartz tube rim for a chosen CO_2 dilution in the fuel stream. The air flow rate is then increased or decreased, so that the flame flashback arises either from the fuel rich or the fuel lean equivalence ratio, respectively. The steps with which the air flow rate is varied was adapted in order to achieve an adequate, repeatable, resolution of the flame flashback. Indeed, for each flow-meter, these steps are always smaller that 1 % of the corresponding full scale. The time interval between those flow rate steps was also larger for smaller flow rates, so that several flow residence times within the tube were allowed for before changing the flow rate. For a range of equivalence ratios at the vicinity of stoichiometry the flame may stabilise in a configuration in which a partial entrance in the tube is observed [1]. In this work flashback is assumed to occur only when the flame visually propagates upstream in the tube, and such a partial entrance was not annotated. The set of experiments enables to determine the critical velocity gradient [$g_c = 32\,\dot{V}/(\pi D^3) = 8\bar{U}/D$], where $\dot{V}$ and $\bar{U}$ are the measured mixture volume flow rate and the corresponding mean flow velocity when flashback occurs, which are functions of the equivalence ratio, ϕ, and fuel (methane or propane) dilution by CO_2. All experiments have been conducted under ambient conditions, i.e., 1 atm and 25 C, and that the tube wall temperature was not measured.

Note that early studies [14, 15] examined the influence on the flame flashback of preheating the fuel/air mixtures. The experimental conditions are such that the preheating temperature does not increase beyond 620 K, the fuels considered are methane and propane. These studies determined that the flame flashback critical velocity gradient increases with the mixture preheating, and that the penetration distance, obtained by dividing the flame speed by the critical velocity gradient, [Eq. (1)] decreases with preheating. More precisely, for a propane/air mixture temperature of 306 K, the penetration distance is 0.8 mm, 0.6 mm and 0.7 mm for the equivalence ratios of 0.8, 1.2 and 1.3, respectively, whereas for 617 K of initial temperature, the values of 0.6 mm, 0.4 mm and 0.5 mm were obtained for equivalence ratios of 0.9, 1.15 and 1.4 [15].

2.2 Laminar flame properties determination

In order to determine Da via Eq. (2), S_L^0, the laminar flame front speed at which the flat, isobaric, adiabatic flame freely propagates must be provided. To this end, numerical calculations were performed using the Ansys CHEMKIN software, version 2020 R1. The chemical kinetic mechanisms adopted were: (1) the GRI-Mech 3.0 mechanism [16] for the methane/air/CO_2 mixtures, and (2) for propane/air/CO_2 mixtures the San Diego Mech [17]. These mechanisms were chosen to represent the chemical kinetics of the studied mixtures based on their predictive ability demonstrated in previous review works [18, 19], a brief

analysis of the influence of different chemical mechanisms is given below. For the sake of conciseness the computed flame velocities are not reported here, but are given in the form of polynomial fits in the supplementary material file.

The classical flame flashback analysis defines the flame thickness, δ_L, as the ratio of the fresh gases mixture thermal diffusion coefficient and the flame speed,

$$\delta_{L,T} = \frac{\alpha}{S_L^0}, \tag{4}$$

thus leading from Eq. (2) to Eq. (3). In this work the computed flame thickness was also determined using a correction to $\delta_{L,T}$ that accounts for variable thermal properties across the flame [20],

$$\delta_{L,B} = 2\frac{\alpha}{S_L^0}\left(\frac{T_b}{T_u}\right)^{0.7}, \tag{5}$$

and the temperature derivative maximum [21], i.e,

$$\delta_{L,max} = \frac{T_b - T_u}{\max\left(dT/dx\right)}, \tag{6}$$

where, T_b and T_u are the temperatures of the burned gases at equilibrium and of fresh mixture, respectively, and dT/dx was obtained from the premixed flame computations. When performing such flame computations care was taken to check for domain and mesh independence of the results for all studied fuel/dilutant/air mixtures.

In order to examine the influence of the chemical mechanism choice, the computed values of the $S_L^0/\delta_{L,max}$ are compared in Fig. 3 for undiluted fuel/air mixtures as a function of the equivalence ratio. This inverse of a characteristic chemical time is given since it appears in Eq. (2). For methane-air mixtures were used the GRI 3.0 [16], San Diego Mech [17], and USC II Mech [22], whereas for propane/air mixtures the latter two have been considered only. Concerning the methane/air mixtures first, Fig. 3a shows that the agreement between the three examined mechanisms is very good for both lean and rich mixtures. The largest discrepancies arise at slightly fuel rich conditions. Indeed, the maximum value predicted with the GRI 3.0 is 905 s^{-1}, which may be compared to 830 and 810 s^{-1} for the San Diego and USC II mechanisms, respectively. These values correspond to 8% and 13% discrepancies between the GRI 3.0 and the two other mechanisms results. As it may be verified in Fig. 3b the discrepancies between the results obtained for propane/air mixtures are larger for lean and near stoichiometric values of ϕ, but very small for rich mixtures. More precisely, the maximum $S_L^0/\delta_{L,max}$ value predicted by the San Diego mechanism is 1152 s^{-1}, whereas the USC II Mech yields 1058 s^{-1}, which represents an 11% difference. As a consequence, considering the fuel/air mixtures studied, the maximum discrepancy related to these chemical kinetic mechanism choices is of the order of 10%.

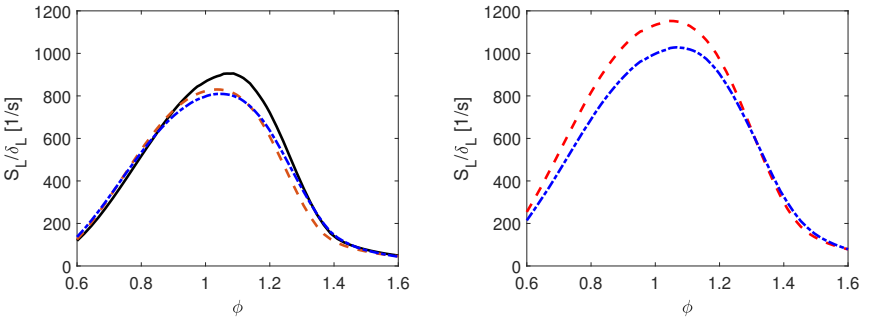

(a) Methane/air (b) Propane/air

Fig. 3: Inverse of the flame characteristic chemical time scale $S_L^0/\delta_{L,max}$ obtained for undiluted mixtures as a function of equivalence ratio. Comparison between chemical kinetic mechanism: GRI 3.0 [16] (solid line), San Diego Mech [17] (dashed line) and USC II Mech [22] (doted line).

The Damköhler number is determined here using both experimental and computed data as $Da = DS_L^0/(8\bar{U}\delta_L) = \pi D^3 S_L^0/(32\dot{V}\delta_L)$. Therefore, the maximum experimental errors associated to Da are 2.4 % and 4.0 % for methane/air and propane/air respectively, whereas those corresponding to ϕ are 1.1 % and 1.8 %. These errors stem from those associated to the tube diameter and reactants flow rates measurements, which differ for methane and propane mixtures due to the different velocity gradients leading to flashback.

In order to recover either the critical velocity gradient, g_c, or the bulk flow velocity, $\bar{U}$, leading to flame flashback, the values of S_L^0 and δ_L must be known. Accordingly, are given as tables, in the supplementary material file, the polynomial coefficients corresponding to the fits of flame speed (S_L^0) and thickness ($\delta_{L,max}$) as a function of equivalence ratio and CO_2 dilution. These should enable a reconstruction of either the critical velocity gradient, g_c, or the flow bulk velocity leading to flashback, $\bar{U}$.

Concerning the mixture composition influence on Da, two different representations are adopted here, i.e., (1) the equivalence ratio of the fresh gases, and (2) their effective Lewis number. The effective Lewis number is determined using a formulation [23] that relies on the Zel'dovich number to continuously vary between the fuel lean and fuel rich limits,

$$Le = Le_1 + H(Le_2 - Le_1), \tag{7}$$

where Le_2 and Le_1 are the fuel-rich and oxidiser-rich Lewis numbers, which are defined as the ratio between the mixture thermal diffusivity, and the diffusion coefficient of the limiting reactant, i.e., fuel in the fuel-lean and oxygen in the fuel rich mixtures. The CO_2 dilution effect is thus accounted for in the thermal diffusion coefficient. These transport coefficients are determined using

the classical formulations available in chemkin. In Eq. (7) H is given by:

$$H = n\frac{G(m, n-1, A)}{G(m, n, A)}, \quad G(m, n, A) = \int_0^\infty \xi^m (\xi + A)^n \exp(-\xi)\, \mathrm{d}\xi, \tag{8}$$

m and n are the orders of reaction with respect to the deficient and abundant reactants, respectively, the normalised final concentration of the abundant reactant is either $A = \beta(\phi - 1)/Le_2$ or $A = \beta(\phi - 1)/Le_1$, and $\beta = E_a(T_b - T_u)/(RT_b^2)$ is the Zel'dovich number. For the sake of simplicity it is assumed that $m = n = 1$; note that different reaction orders would lead to different slopes of the $Le(\phi)$ curve [Eq. (7)]. It should be stressed that this equation was derived on the basis of a single-step Arrhenius reaction, which in turn leads to the Eq. (8) reactant mass fraction dependency of the effective Lewis number. Therefore, when using such a formulation to determine Le, the detailed chemistry effects that may arise due to the CO_2 influence are not accounted for.

The Lewis number values for fuel lean (Le_1, which corresponds to $\phi \to 0$) and fuel rich mixtures (Le_2, which corresponds to $\phi \to \infty$) diluted by CO_2 are given in Tab. 1. In this table each column corresponds to a chosen CO_2 dilution in the fuel, ranging from 0% to 75%, and each line gives (Le_1, Le_2) pairs for a given fuel/air mixture. These Lewis number limit values were computed using the transport properties obtained with the classical multi-component mixture formulas. In this table it may be verified that the CO_2 dilution in the fuel leads, in methane/air rich mixtures, to a decrease of the Le_2 values which is associated to the smaller thermal diffusivity of CO_2. On the contrary, the propane/air mixtures are characterised by a Le_2 increasing trend with CO_2 dilution, which is due to the propane thermal diffusivity being smaller than that of the CO_2. Since the CO_2 dilution is effected in the fuel, the lean limit values (Le_1) are unaffected, because the thermal diffusivity is that of the air.

Table 1: Lewis number values for fuel lean ($\phi \to 0$) and rich ($\phi \to \infty$) mixtures, noted (Le_1, Le_2), for different CO_2 (%) dilutions.

	CO_2 (%) in fuel			
	0	25	50	75
Methane/air	(0.997, 1.09)	(0.997, 1.01)	(0.997, 0.92)	-
Propane/air	(1.93, 0.82)	(1.93, 0.85)	(1.93, 0.97)	(1.93, 1.14)

The Zel'dovich number is determined using a recently proposed methodology, which uses an extended Arrhenius expression that is optimally fitted to the computed premixed flame heat release rate [24]:

$$\dot{q}(\theta) \propto \{1 - \exp[\beta'(1 - 1/\theta)]\}^{\beta''} \exp\left\{\frac{\beta(\theta - 1)}{(1 + \gamma\theta)/(1 + \gamma)}\right\}, \tag{9}$$

where $\theta = (T - T_u)/(T_b - T_u)$ is the temperature based reaction progress variable, and $\gamma = (T_b - T_u)/T_u$ represents the thermal expansion across the flame. In this heat release rate expression, β' and β'' control, respectively, the initial and the final $\dot{q}$ decrease towards equilibrium as $\theta \to 1$. For the sake of completeness, the Zel'dovich number correlations resulting from such a procedure that are used in Eq. (8) read:

$$\text{methane/air} : \beta = 10.4\,\phi^4 - 49.6\,\phi^3 + 98.7\,\phi^2 - 90.7\,\phi + 33.4, \tag{10}$$

$$\text{propane/air} : \beta = -21.7\,\phi^4 + 106\,\phi^3 - 164\,\phi^2 + 94.2\,\phi - 12.3, \tag{11}$$

for which $R^2 > 0.98$.

3 Results and Discussion

The flame flashback results obtained for the methane and propane CO_2 diluted mixtures with air are now presented. These results considered dilutions ranging from 0% to 50% for methane, and from 0% to 75% for propane. In order to cover the equivalence ratio range between the lean and the rich flashback limits the tube diameters used are $D = 4, 5, 6$ and 17 mm. These lean and rich flashback limits are found for equivalence ratios of $\phi \approx 0.7$ and ≈ 1.3 and of $\phi \approx 0.7$ and ≈ 1.6 for methane and propane mixtures, respectively. Given these equivalence ratio ranges and tube diameters, the associated bulk flow velocities and total flow rates range from $0.025 < \bar{U} < 1.47$ m/s and $0.0192 < \dot{\forall}_t < 21.45$ lpm, respectively. For a given tube diameter, the equivalence ratio range is typically covered by determining circa 500 critical flashback conditions.

In what follows are examined the influences on the critical flashback Damköhler number of (i) the flame thickness definition, (ii) the mixture equivalence ratio and fuel dilution by CO_2 and (iii) the Lewis number.

3.1 Flame thickness definition influence

In this section is examined the influence of three different flame thickness definitions on the flame flashback critical Damköhler number, Eq. (2). More specifically, the considered flame thickness definitions are given by Eqs. (4), (5) and (6). Figure 4 shows the evolution with the mixture equivalence ratio of the computed flame thickness, as well as the corresponding critical Damköhler numbers, for methane/air and propane/air mixtures. This particular (ϕ, Da) representation was chosen due to its interest to process safety. For the sake of simplicity undiluted fuel mixtures results are given and discussed in this section only.

In Figs. 4a and 4b it can clearly be seen that the three flame thickness definitions lead to minimum values at equivalence ratios slightly larger than stoichiometry, which is related to the well-known rich shift of maximum S_L^0 [25]. Indeed, regardless of the flame thickness definition chosen, both methane and propane mixtures with air exhibit a thickness increase for leaner

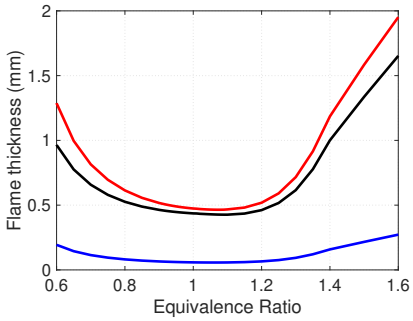

(a) Flame thickness, methane/air

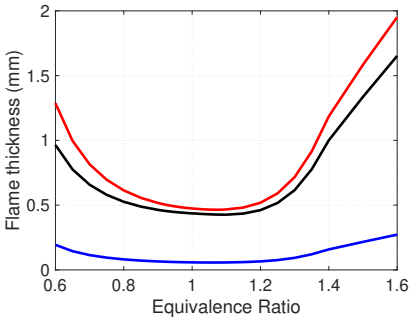

(b) Flame thickness, propane/air

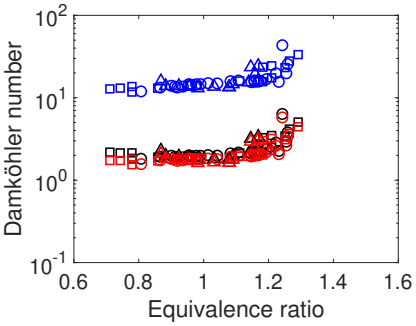

(c) Damköhler number, methane/air

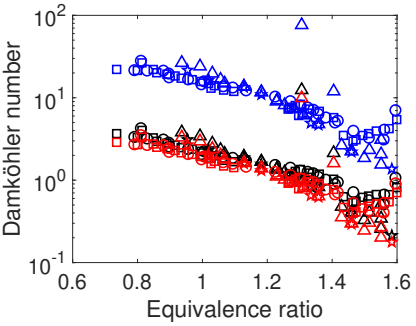

(d) Damköhler number, propane/air

Fig. 4: Flame thickness and Damköhler number as a function of the equivalence ratio for undiluted fuel/air mixtures, $\delta_{L,T}$: blue, $\delta_{L,B}$: red, $\delta_{L,max}$: black. The symbols correspond to different tube diameters, i.e., $D = 4$ ($\triangle$), 5 ($\star$), 6 ($\circ$) and 17 ($\square$) mm.

and richer mixtures. For instance, the leanest methane/air flame thermal thickness is 3.3 times that of a stoichiometric flame, whereas this ratio is 2.2 when the maximum temperature gradient thickness is considered. Concerning lean propane/air flames, these ratios are somewhat smaller, i.e., 2.5 and 1.8, respectively. Rich fuel/air mixtures exhibit similar trends, albeit with larger absolute values for this thickness ratio. Moreover, at stoichiometry, the flame thickness values computed via Eqs. (4), (5) and (6), i.e., $\delta_{L,T}, \delta_{L,B}$, and $\delta_{L,max}$, are respectively 0.058, 0.47, and 0.43 mm for methane/air and 0.051, 0.42, and 0.36 mm for propane air mixtures. This reasonable agreement between $\delta_{L,max}$ and $\delta_{L,B}$ is verified throughout the considered equivalence ratio range, which confirms that the latter is a good approximation to the former.

Furthermore, Figs. 4a and 4b indicate that the choice of flame thickness definition should exert a significant impact on the Damköhler number computed via Eq. (2), since $\delta_{L,T} \ll \delta_{L,max}$. Indeed, Figs. 4c and 4d clearly show

that the critical Damköhler number computed using the flame thermal thickness is an order of magnitude larger than that resulting from the two other formulations. For example, stoichiometric methane and propane air mixtures exhibit Damköhler number values of 1.97 and 2.06, respectively, when $\delta_{L,max}$ is used, whereas the values corresponding to δ_T are 0.43 mm and 0.37 mm. Nevertheless, the overall trend with the mixture equivalence ratio is independent of the flame thickness definition. For instance, examining first the computed Da values using $\delta_{L,max}$ as flame thickness definition, for methane mixtures, Fig. 4c shows that the Damköhler number is practically independent of the equivalence ratio for $0.7 \leq \phi \leq 1.1$, that is, $Da \approx 2.5$, when $\delta_{L,max}$ is chosen. However, for $\phi > 1.1$, an increase in the Damköhler number with equivalence ratio is observed. Using the same thickness definition for undiluted propane mixtures, as seen in Fig. 4d, the Damköhler number decreases steadily from ≈ 4 to ≈ 0.2 with ϕ, to $0.7 \leq \phi \leq 1.5$. These results confirm early numerical results [6], which indicated that the constant Da assumption should not be used to describe flame flashback. However, methane/air and propane/air mixtures exhibit increasing and decreasing Da trends with ϕ, respectively, which discussion is deferred to section 3.3

3.2 Equivalence ratio and CO_2 dilution influence

The results of the critical Damköhler number for mixtures of methane/air/-CO_2 and propane/air/CO_2 are presented in Fig. 5, which depicts the Da values as a function of the equivalence ratio, for several tube diameters. Since

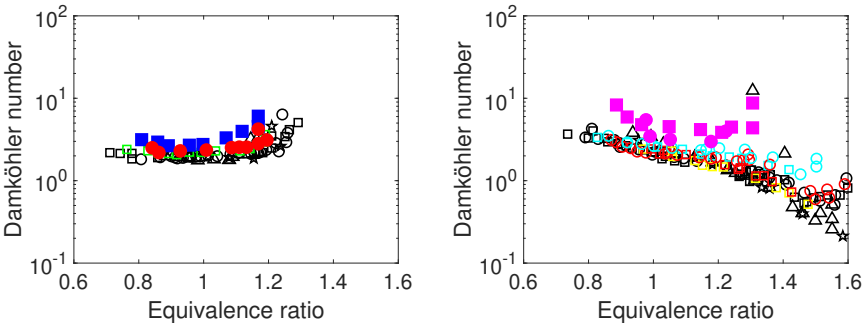

(a) Methane/air (b) Propane/air

Fig. 5: Flashback Damköhler number for methane and propane/air flames diluted with CO_2 as a function of the equivalence ratio for mixtures in tubes of $D = 4$ (△), 5 (⋆), 6 (○) and 17 (□) mm. The symbols colours are organised such as: black - undiluted, green - 10 %, yellow - 15 %, red - 25 %, blue - 30 %, cyan - 50 % and magenta - 75 %. The filled symbols represent the highest dilution percentage.

the three flame thickness definitions examined in section 3.1 yielded analogous trends, the one adopted here is $\delta_{L,max}$ only. Note that in the absence of detailed chemical kinetics computational results, which could be the case for fuel mixtures for which the combustion chemistry is unknown, using $\delta_{L,B}$ instead seems fair. Figure 5 shows that, for moderate CO_2 dilutions, the overall trends of Da with ϕ are identical to those seen in Fig. 4 for undiluted mixtures, i.e., for methane/air mixtures a moderate Da increase with ϕ is seen, whereas propane/air mixtures exhibit a corresponding decrease that spans over more than an order of magnitude. Since the adopted model uses the assumption that $Da = \delta_p/\delta_L$, this suggests that, for a given δ_L, flame penetration distance is relatively larger in leaner propane/air mixtures, when compared to richer ones, which is agreement with the early findings discussed in section 2.1 [14, 15].

Concerning now the higher CO_2 dilutions, as seen in Fig. 5a, methane mixtures exhibit a Da increase as CO_2 is added beyond 30 %. For example, in the $D = 17$ mm tube, for stoichiometric methane/air mixtures, the Damköhler number is close to 2 and for methane/air/30%CO_2 mixtures it is nearly 3. As may be seen in Fig. 5b propane mixtures have a similar behaviour with respect to CO_2 dilution. Indeed, a stoichiometric propane/air mixture characterised by a Damköhler number of the order of 2, whereas a stoichiometric mixture of propane/air/75 % CO_2 is of the order of 4. It should be stressed that, in the particular case of those highest fuel dilutions, and for the smallest tube diameters, the flame flashback is followed by a nearly immediate extinction, i.e., the flame does not sustain stable propagation throughout the tube length. In this sense, these particular conditions do not strictly represent the flame flashback phenomenon. Thus, if those flame extinction results are discarded, Fig. 5 indicates that the critical Da value is independent of the tube diameter regardless the CO_2 dilution considered. As a consequence, for a given equivalence ratio – and thus a Damköhler number – regardless the dilution by CO_2, the flashback bulk velocity is such that $\bar{U} \propto DS_L^0/(8\delta_{L,max})$.

In order to further quantify the CO_2 dilution effect, Tab. 2 reports the critical Damköhler number values for stoichiometric fuel/air mixtures and the different dilutions used. The overall Da increasing trend with CO_2 fuel dilution is clearly seen. For instance, for methane and propane mixtures the critical Da value increases by 40% and 67%, when the respective dilutions are 30% and 75%. Note that the empty boxes in this table are dilutions for experiments have not been performed.

Table 2: Damköhler number values for stoichiometric fuel/air mixtures and different fuel dilutions.

	CO_2 in fuel						
	0	10	15	25	30	50	75
Methane	1.97	2.20	-	2.35	2.75	-	-
Propane	2.06	-	2.41	2.42	-	2.56	3.45

3.3 Lewis number and CO_2 dilution influence

In order to address the relation between the Lewis number and the critical flashback conditions, Fig. 6 depicts the effective Lewis number for the different combustible mixtures studied. This figure shows that the effective Lewis

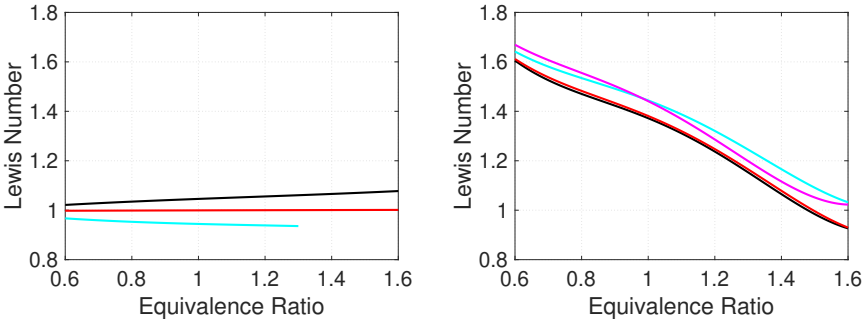

(a) Methane/air (b) Propane/air

Fig. 6: Computed effective Lewis number as a function of the mixture equivalence ratio for different CO_2 dilutions in the studied fuels. The symbols colours are organised such as: black - undiluted, red - 25 %, cyan - 50 % and magenta - 75 %.

number behaviour as a function of equivalence ratio is a classical one, tending to the value of the limiting reactant for very lean or very rich mixtures. Concerning fuel-rich mixtures first, the increase of CO_2 dilution in the fuel leads to a decrease of the effective Lewis number for methane mixtures, whereas an increase is observed for propane mixtures; these tendencies are related to the Le_2 values in Tab. 1. However, dilution by CO_2 exerts a less pronounced negligible influence on the effective Lewis number of lean propane mixtures, which is associated to the Le_1 values given in Tab. 1.

Figure 7 depicts the critical Damköhler number as a function of the effective Lewis number for the different mixtures studied. The present results are shown as symbols, whereas the lines represent those of previous numerical studies [8]. Again, each symbol represents a tube diameter, whereas the colours stand for different fuel dilutions by CO_2. It is important to stress that these solid and dashed lines represent limiting cases of isothermal (300 K) and adiabatic boundary conditions at the tube wall, respectively, and that the Zel'dovich number used in the depicted computational results is $\beta = 10$ [8]. Note that these computational results used Eq. (3) to define the Damköhler number. Therefore, in order to provide for a fair comparison with the present experimental values, these computed Da values were corrected using $\delta_{L,T}/\delta_{L,B} = 1/7.55$ from Eqs. (4) and (5). These computational results clearly show that the flame flashback Da increases with the Lewis number and decreases when the tube

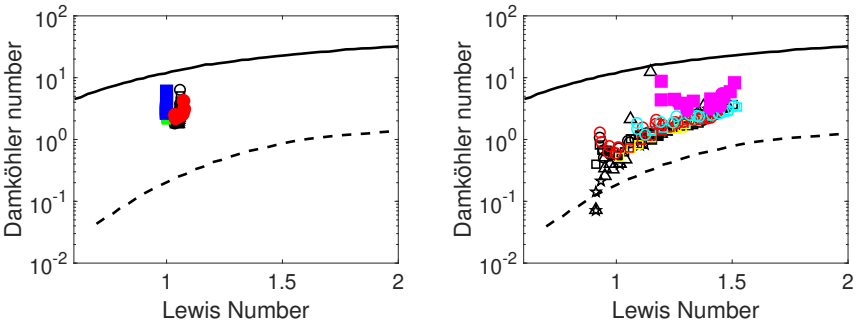

(a) Methane/air (b) Propane/air

Fig. 7: Flashback Damköhler number for methane and propane/air flames diluted with CO_2 as a function of the effective Lewis number for mixtures in tubes of $D = 4$ (△), 5 (⋆), 6 (○) and 17 (□) mm. The symbols colors are organized such as: black - undiluted, green - 10 %, yellow - 15 %, red - 25 %, blue - 30 %, cyan - 50 % and magenta - 75 %. The filled symbols represent the highest dilution percentages. The lines correspond to the previously computed results [8]: dashed - adiabatic, solid - isothermal (300 K) tube wall.

wall approaches an adiabatic condition: for instance, at stochiometry the computed Da is close to 12 when the tube wall is assumed to be isothermal, and $\approx .21$ when an adiabatic surface is prescribed. The actual thermal boundary conditions prevailing at the experiments should lie between those limiting situations.

An increasing trend of $Da(Le)$ was also observed in the present study for propane/air flames results, as may be verified in Fig. 7b, which closely follow the adiabatic boundary tendency, with the notable exception of those flashback cases that lead to flame extinction (solid symbols) – that are characterised by larger critical Damköhler number values. Indeed, within the range of the current measured data, the following correlation holds:

$$Da \propto Le^{\ell}, \quad \text{with } \ell = 5.06, \tag{12}$$

which may be compared with a previously determined value of $\ell = 1.68$ [9] for turbulent hydrogen/air flames. Notice that close to the tube wall, near the flame base, non-unity Lewis number effects should influence the flame speed and thickness, which values could be different than those given by 1D planar freely propagating simulations. The critical Damköhler number correlation determined thus inherently incorporates such effect. Unfortunately the experimental techniques used do not permit to isolate curvature or stretch effects on Da, which can be done in detailed numerical simulations [26–28].

The observed methane/air mixtures behaviour seen in Fig. 7a could seem, at first, to contradict that of the propane/air mixtures. However, for these

mixtures, which are characterised by a rather small Lewis number variation, the effect dominating the critical Da seems to be that of the thermal boundary condition at the tube wall. Indeed, when using this (Le, Da) representation, Fig. 7a results indicates that smaller tube diameters tend to lead to larger Da values, which was not readily apparent in Fig. 5a, which used a (ϕ, Da) depiction. For these smaller tubes, the ratio between the quenched mixture region and flame surface area could be expected to increase, thus influencing the flashback conditions. These results underscore the need to include, in the Da model, a Péclet number, which could be modelled as [29] $Pe = \delta_q/\delta_L = 1/\varphi - 1$, where the quenching distance, δ_q, is schematically shown in Fig. 1, and φ is the ratio between the measured flame heat transfer to the wall and the flame heat release. Developing a flame flashback model that accounts for flame quenching by the wall – via a Péclet number – should lead to better predictions, since it would involve the length scale corresponding to the quenching phenomenon which length scale (δ_q), as shown in Fig. 1, may be expected to be different from that of the flashback (δ_p). However, the present experimental apparatus does not enable a direct measurement of the former, and thus of φ. Therefore the development of a more general correlation, i.e, $Da(Le, Pe)$ is out of reach of the present endeavour. Another interesting avenue for such a development could be the use of artificial neural networks to avoid systematic measurements of the tube tip thermal boundary conditions [30].

4 Conclusion

The critical Damköhler number for flame flashback to occur in CH_4 and C_3H_8 mixtures was determined as a function of the fuel, the equivalence ratio and CO_2 dilution. To this end, measured flashback critical velocity gradient data, which provides a fluid time scale, was combined with detailed chemical kinetics simulation results of laminar one-dimensional, freely propagating premixed flames. These computations enabled to define the flame characteristic time scale using, together with the laminar flame speed, three different flame thickness definitions, i.e., (i) the classical thermal thickness, (ii) that based on the maximum temperature gradient, and (iii) one that corrects for temperature dependence of the thermal diffusion coefficient in (i) and thus approximates (ii). These length scales led to critical Damköhler numbers that exhibit a similar trend with equivalence ratio, but which value is nearly an order of magnitude larger when (i) is used. The critical Damköhler number definition eventually adopted is that based on the maximum temperature gradient, which has the advantage of accounting for detailed chemistry and transport formulations.

Methane/air/CO_2 flames exhibited an increasing Damköhler number with equivalence ratio. On the other hand, propane/air/CO_2 flashback is characterised by almost a two order of magnitude Damköhler number decrease as the equivalence ratio goes from 0.7 to 1.6. For both mixtures, CO_2 dilution results

in a Damköhler number increase when flashback leads to flame extinction within the tube only.

The Lewis number influence on the critical Damköhler number of propane mixtures was found to follow existing numerical simulation results trends, leading to a $Da \propto Le^{5.06}$ dependency. This good agreement between the present results and those numerical simulations suggest that the critical Damköhler number defined using the temperature gradient flame thickness is more suitable than the one that uses the thermal thickness. On the contrary, methane mixtures results showed a lesser sensitivity to Lewis number variations – which are rather small – but a seemingly larger one to tube diameter. Indeed, smaller tube diameters led to larger critical Damköhler number values, approaching those of the constant tube temperature simulations, which could be related to the thermal boundary conditions at the wall, that were not characterised in this study. Such a result indicates that the quenching region near the flame wall should be accounted for in a more general Damköhler number model, which could use a Péclet number, for instance.

5 Acknowledgments

This work was performed while L.F. Figueira da Silva was on leave from the Institut Pprime (UPR 3346 CNRS, France). This work was supported by Petrobras contract no. 5900.0111688.19.9 under the technical monitoring of Dr. P. R. Pagot. Support was also received from Conselho Nacional de Desenvolvimento Científico e Tecnológico (CNPq, Brazil) under the Research Grant No. 304444/2018-9. This study was financed in part by the Coordenação de Aperfeiçoamento de Pessoal de Nível Superior - Brasil (CAPES) - Finance Code 001.

Ethical statement

- Funding: Maria Clara de Jesus Vieira received funding from Petroleo Brasileiro SA (grant 5900.0111688.19.9) and from Coordenação de Aperfeiçoamento de Pessoal de Nível Superior, Finance Code 001. Luis Fernando Figueira da Silva received funding from Petroleo Brasileiro SA (grant 5900.0111688.19.9), from Coordenação de Aperfeiçoamento de Pessoal de Nível Superior, Finance Code 001 and from Conselho Nacional de Desenvolvimento Científico e Tecnológico, (grant 304444/2018-9).
- Conflict of Interest: The authors have no competing interests to declare that are relevant to the content of this article.
- Ethical approval: not applicable.
- Informed consent: not applicable.
- Author contribution: All authors contributed to the study conception and design. Material preparation, data collection and analysis were performed by Maria Clara de Jesus Vieira and Luis Fernando Figueira da Silva. The first draft of the manuscript was written by Luis Fernando Figueira da Silva and

Maria Clara de Jesus Vieira, and all authors commented on previous versions of the manuscript. All authors read and approved the final manuscript.

References

[1] Lewis, B., von Elbe, G.: Combustion, Flames and Explosions of Gases. Academic Press, Orlando, FL (1987)

[2] Kalantari, A., McDonell, V.: Boundary layer flashback of non-swirling premixed flames: Mechanisms, fundamental research, and recent advances. Prog. Energy Combust. Sci. **61**, 249–292 (2017). https://doi.org/10.1016/j.pecs.2017.03.001

[3] Gruber, A., Chen, J.H., Valiev, D., Law, C.K.: Direct numerical simulation of premixed flame boundary layer flashback in turbulent channel flow. J. Fluid Mech. **709**, 516–542 (2012). https://doi.org/10.1017/jfm.2012.345

[4] Eichler, C., Sattelmayer, T.: Premixed flame flashback in wall boundary layers studied by long-distance micro-piv. Exp. Fluids **52**, 347–360 (2012). https://doi.org/10.1007/s00348-011-1226-8

[5] Lewis, B., von Elbe, G.: Stability and structure of burner flames. J. Chem. Phys. **11**, 75–97 (1943). https://doi.org/10.1063/1.1723808

[6] Kurdyumov, V.N., Fernández, E., Liñán, A.: Flame flashback and propagation of premixed flames near a wall. Proc. Combust. Inst. **28**, 1883–1889 (2000). https://doi.org/10.1016/S0082-0784(00)80592-5

[7] Kurdyumov, V.N., Fernández-Tarrazo, E.: Lewis number effect on the propagation of premixed laminar flames in narrow open ducts. Combust. Flame **128**, 382–394 (2002). https://doi.org/10.1016/S0010-2180(01)00358-3

[8] Kurdyumov, V., Fernández-Tarrazo, E., Truffaut, J.-M., Quinard, J., Wangher, A., Searby, G.: Experimental and numerical study of premixed flame flashback. Proc. Combust. Inst. **31**, 1275–1282 (2007). https://doi.org/10.1016/j.proci.2006.07.100

[9] Kalantari, A., Sullivan-Lewis, E., McDonell, V.: Flashback propensity of turbulent hydrogen–air jet flames at gas turbine premixer conditions. J. Eng. Gas Turbines Power **138**, 061506 (2016). https://doi.org/10.1115/1.4031761

[10] Hoferichter, V., Hirsch, C., Sattelmayer, T.: Prediction of boundary layer flashback limits of laminar premixed jet flames. Proceedings of the ASME Turbo Expo **4A-2018**, 1–11 (2018). https://doi.org/10.1115/

GT201875546

[11] Ebi, D., Bombach, R., Jansohn, P.: Swirl flame boundary layer flashback at elevated pressure: Modes of propagation and effect of hydrogen addition. Proc. Combust. Inst. **38**, 6345–6353 (2021). https://doi.org/10.1016/j.proci.2020.06.305

[12] Novoselov, A.G., Ebi, D., Noiray, N.: The effect of hydrogen addition on confined turbulent boundary layer flashback studied with a critically strained flame model. In: AIAA SCITECH 2022 Forum, pp. 1–6. American Institute of Aeronautics and Astronautics, ??? (2022). https://doi.org/10.2514/6.2022-1739

[13] Grosseuvres, R., Comandini, A., Bentaib, A., Chaumeix, N.: Combustion properties of $H_2/N_2/O_2$/steam mixtures. Proc. Combust. Inst. **37**, 1537–1546 (2019). https://doi.org/10.1016/j.proci.2018.06.082

[14] Grumer, J., Harris, M.E.: Temperature dependence of stability limits of burner flames. Ind. Eng. Chem. **46**, 2424–2430 (1954)

[15] Dugger, G.L.: Flame stability of preheated propane-air mixtures. Ind. Eng. Chem. **47**, 109–114 (1955)

[16] Smith, G.P., Golden, D.M., Frenklach, M., Moriarty, N.W., Eiteneer, B., Goldenberg, M., Bowman, C.T., Hanson, R.K., Song, S., Gardiner, W.C., Lissianski, V.V., Qin, Z.: GRI-Mech 3.0. http://www.me.berkeley.edu/gri{_}mech/

[17] Chemical-Kinetic Mechanisms for Combustion Applications, San Diego Mechanism web page, Mechanical and Aerospace Engineering (Combustion Research), University of California at San Diego. http://combustion.ucsd.edu

[18] Konnov, A.A., Mohammad, A., Kishore, V.R., Kim, N.I., Prathap, C., Kumar, S.: A comprehensive review of measurements and data analysis of laminar burning velocities for various fuel+air mixtures. Prog. Energy Combust. Sci. **68**, 197–267 (2018). https://doi.org/10.1016/j.pecs.2018.05.003

[19] Mendoza Orbegoso, E.M., Figueira da Silva, L.F., Novgorodcev Junior, A.R.: On the predictability of chemical kinetics for the description of the combustion of simple fuels. J. Braz. Soc. Mech. Sci. Eng. **33**, 492–505 (2011). https://doi.org/10.1590/S1678-58782011000400013

[20] Blint, R.: The relationship of the laminar flame width to flame speed. Combust. Sci. Technol. **49**, 79–92 (1986). https://doi.org/10.1080/00102208608923903

[21] Poinsot, T., Veynante, D.: Theoretical and Numerical Combustion, p. 522. R.T. Edwards Inc., ??? (2005)

[22] Wang, H., You, X., Joshi, A.V., Davis, S.G., Laskin, A., Egolfopoulos, F., Law, C.K.: USC Mech Version II. High-Temperature Combustion Reaction Model of H2/CO/C1-C4 Compounds. http://ignis.usc.edu/USC_Mech_II.htm

[23] Joulin, G., Mitani, T.: Linear stability analysis of two-reactant flames. Combust. Flame **40**, 235–246 (1981). https://doi.org/10.1016/0010-2180(81)90127-9

[24] de Jesus Vieira, M.C., Figueira da Silva, L.F.: Premixed flame heat release single-step chemistry for H_2, CH_4, and C_3H_8 mixtures. J. Braz. Soc. Mech. Sci. Eng. **44**(131), 1–16 (2022). https://doi.org/10.1007/s40430-022-03437-7

[25] Law, C.K., Makino, A., Lu, T.F.: On the off-stoichiometric peaking of adiabatic flame temperature. Combust. Flame **145**, 808–819 (2006). https://doi.org/10.1016/j.combustflame.2006.01.009

[26] Howarth, T.L., Aspden, A.J.: An empirical characteristic scaling model for freely-propagating lean premixed hydrogen flames. Combust. Flame **237**, 111805 (2022). https://doi.org/10.1016/j.combustflame.2021.111805

[27] Berger, L., Attili, A., Pitsch, H.: Intrinsic instabilities in premixed hydrogen flames: Parametric variation of pressure, equivalence ratio, and temperature. part 1 - dispersion relations in the linear regime. Combust. Flame **240**, 111935 (2022). https://doi.org/10.1016/j.combustflame.2021.111935

[28] Berger, L., Attili, A., Pitsch, H.: Intrinsic instabilities in premixed hydrogen flames: parametric variation of pressure, equivalence ratio, and temperature. part 2 – non-linear regime and flame speed enhancement. Combust. Flame **240**, 111936 (2022). https://doi.org/10.1016/j.combustflame.2021.111936

[29] Boust, B., Sotton, J., Labuda, S.A., Bellenoue, M.: A thermal formulation for single-wall quenching of transient laminar flames. Combust. Flame **149**, 286–294 (2007). https://doi.org/10.1016/j.combustflame.2006.12.019

[30] Leask, S.B., McDonell, V.G., Samuelsen, S.: Neural network prediction of boundary layer flashback. J. Eng. Gas Turbines Power **143**, 1–6 (2021). https://doi.org/10.1115/1.4049987